Advanced Mathematical Models & Applications
Vol.8, No.2, 2023, pp.199-222

HOMOTOPY ANALYSIS METHOD FOR FRACTIONAL DERIVATIVE MODEL OF ENERGY GENERATION IN THE HUMAN CELL

C.L. Ejikeme, D.F. Agbebaku*, M.B. Okofu, M.I. Atuokwu, C. Okoye

Department of Mathematics, University of Nigeria, Nsukka, Nigeria

Abstract. The human body require energy for mechanical activities. This energy is obtained from the food we eat and they are stored in the human body in chemical form as Carbohydrates, Protein and Fats. In the event that energy is needed in any part of the body, the chemical energy is transformed into utilizable energy form as Adenosine Triphosphate (ATP) and transported to places within the cells where they are needed. This is in some ways similar to the energy generation in the diesel engine of an automobile. In this paper, the mathematical equation governing the generation of energy in a diesel engine is modified to produce a mathematical model of energy generation in the mitochondria of human cell. A partial differential equation with boundary conditions, representing the process of energy generation in the human cell, was obtained. The solution to the integer partial derivative mathematical model was first obtained using Homotopy Analysis Method (HAM). Surface plots of the solution obtained by HAM are presented. From the study, the energy generated in the human cells increases with time as the coefficient of diffusion increases and also whenever the control parameter is in the negative side of the convergence region. Furthermore, a fractional-time partial derivative model was also formulated by replacing the integer-time derivative with a fractional derivative in the Caputo sense. The solution to the fractional-time derivative model was also obtained using the Homotopy Analysis Method (HAM) and surface plot of solution are also presented. In comparing the integer-derivative model with that of the fractional derivative model, the energy generated by the integer model seems higher than that of the fractional model. The fractional-time derivative model is a generalization of the integer derivative model. When $\alpha = 1$, the solution of the integer and fractional model coincide. The novelty and contribution of this paper is the formulation of a mathematical model of energy generation in the mitochondria of human cell through the food we eat. Both integer derivative and fractional derivative models were formulated. Approximate analytic solutions to both models were obtained using the Homotopy Analysis Method.

Keywords: Fractional time-derivative, energy generation, human cell, Caputo, Homotopy analysis Method.
AMS Subject Classification: 92-10, 26A33, 31R11, 34A08, 74G10.
***Corresponding author:** Dennis Agbebaku, Department of Mathematics, University of Nigeria, Nsukka, Nigeria, e-mail: *dennis.agbebaku@unn.edu.ng*
Received: 6 November 2022; Revised: 12 May 2023; Accepted: 14 June 2023; Published: 3 August 2023.

1 Introduction

For more than three centuries, fractional calculus has been a veritable tool in the analysis of mathematical models. In recent times, perturbing mathematical models of deterministic integer order differential equation to models written in terms of fractional order derivatives has become a popular area of research (Liu et al., 2020; Tuan et al., 2020) and the reference therein. Fractional order differential equations emanates from fractional order derivatives or integral

How to cite (APA): Ejikeme, C.L., Agbebaku, D.F.,. Okofu, M.B, Atuokwu, M.I., & Okoye, C.O. (2023). Homotopy analysis method for fractional derivative model of energy generation in the human cell. *Advanced Mathematical Models & Applications*, *8*(2), 199-222.

operators. These derivatives or integral operators do not only depend on their current state but also upon all of their past states. This is due to the nonlocal nature of the fractional order derivative as oppose to the integer order derivative which is local in nature (Hoan et al., 2020). The nonlocal nature of fractional derivatives makes these operators very useful and powerful in evaluating the next state of the system. Thus these operators are more efficient than other classical deterministic operators in the analysis mathematical models.

Mathematical models of most physical systems involve either ordinary differential equations (ODE) or partial differential equations (PDEs). In order to know the behavior of the system, the solutions of the governing differential equations need to be investigated. In this regard, there are well-known classical methods for obtaining classical solutions, (see Hastings & McLeod (2011)) for details of some classical methods. However, physical systems occurring in nature comprise of equations with complex geometry for which computation of exact solutions may be difficult or not even possible. In such cases, analytic, semi-analytic or numerical methods are deployed to obtain a solution (Chakraverty et al., 2019). Numerical methods have been very useful in the analysis of models of energy generation in the Engineering field, (Didi et al., 2022; Ghalandari et al., 2019; Nabipour et al., 2020; Molajou et al., 2021; Jafarian-Namin et al., 2019), and the references therein.

Fractional differential equations has been applied in various field like physics, biology, medicine, image processing, optimization, electrodynamics, nanotechnology, biotechnology, and engineering Kilbas et al. (2006); Kumar et al. (2018); Baleanu et al. (2017); Nasrolahpour (2013); Zhang et al. (2012); Yi-Fei (2007); Baleanu et al. (2010); Mainardi (2010); Tarasov & Tarasova (2017); Sun et al. (2018) and the references therein. Converting an integer derivative model to an appropriate fractional derivative model may be easy but obtaining a solution to such a model is known to be very challenging and requires some powerful numerical or analytical techniques. Some of the techniques used, as seen in the literature, includes but not limited to homotopy perturbation method(HPM) (He, 1999; Yildirim, 2009), Laplace transform method (LTM) (Kexue and Jigen, 2011), homotopy analysis method(HAM) (Ejikeme et al., 2018; Akinyemi, 2019; Iyiola, 2015), Adomian decomposition method(ADM) (Ray & Bera, 2005), Differential transformation method(DTM) (Arikoglu and Ozkol, 2007), perturbation-iteration algorithm (Şenol & Dolapci, 2016), iterative Shehu transform method, (Akinyemi & Iyiola, 2020a), residual power series method (Senol, 2020; Kumar et al., 2016; Ahmad, 2015), and q-homotopy analysis transform method in (Akinyemi, 2019; Akinyemi & Huseen, 2020; Akinyemi & Iyiola, 2020b; Kumar et al., 2017).

The energy content of the food we eat exist in chemical form. This chemical energy is stored in the human body as Carbohydrates, Protein and Fats. Human cells require chemical energy for metabolic reactions, to transport substances across its membranes and to do mechanical work, such as moving muscles. When energy is needed in any part of the body, the chemical energy is transformed into utilizable energy form in the form of Adenosine Triphosphate(ATP) and transported to places within the cells where they are needed. The ATP is not a storage molecule for energy but it is an unstable molecules whose bonds are easy to break, making it a useful source of energy for cells (Otugene, 2012; Hickman et al., 1997).

All energy production begins in the Cytosol (Cytoplasm) of the cell. Here, large molecules are catabolized into smaller molecules but very little energy is produced. These smaller molecules are then absorbed and processed in reactions inside the mitochondria. This is known as ATP Cycle. There are three steps in the generation of energy in the form of ATP in the human cells. These are: (i) glycolysis (ii) Kreb's cycle or Citric Acid (TCA)Cycle and (iii) Oxidative phosphorylation.

Glycolysis is a series of biochemical reactions by which one molecule of six-carbon sugar glucose is oxidized to form two molecules of three-carbon pyruvic acid, two molecules each of the energy-carrying molecule ATP and NADH, and two molecules of water. Here, a molecule of glucose is degraded in a series enzyme-catalyzed reactions to yield two molecules of the three

carbon compound pyruvate. In the preparatory phase of glycolysis (that is phase one to five) two molecules of ATP are invested and two triphosphate are obtained. During the sequential reactions or payoff phase of glycolysis, some of the free energy released from glucose is conserved in the form of ATP and NADH. At this phase, four molecules of ATP are produced. Therefore, glycolysis is the oxidation of glucose to pyruvic acid with some ATP and NADH produced (Hickman et al., 1997). The overall process of glycolysis is the following reaction equation

$$Glucose + 2NAD + 2ADP + 2Pi \longrightarrow 2pyruvate + 2NAD + 2ADP + 2H^+ + 2ATP + 2H_2O.$$

In the anaerobic condition(absence of oxygen), homolatic fermentation of pyruvate occurs in the muscles while under aerobic condition(presence of oxygen), pyruvate is oxidized to acetyl-CoA(acetyl Coenzymes A) and this reacts with Oxoloacetate to begin the next stage of ATP production called the Kreb's cycle or citric acid cycle or tricarboxylic acid cycle. Kreb's cycle is the oxidation and decarboxylation of acetylCoA to carbon(iv)oxide with some ATP, NADH and $FADH_2$ produced. Decarboxylation is the first step in the aerobic process of glucose metabolism. This and all subsequent steps (citric Acid Cycle and Electron Transport) will occur only when oxygen is available and takes place inside the mitochondria (Hickman et al., 1997). The equation of decarboxylation is

$$2pyruvateacid + 2NAD^+ + 2CoA \longrightarrow 2AcetylCoA + 2CO_2 + 2NADH.$$

Therefore, the Kreb's Cycle is the part of the aerobic metabolism of glucose which involves eight enzymes reactions occurring in the mitochondrial matrix that reduce the co-enzymes NAD^+ and FAD. Oxidation and decarboxylation reactions occur which catabolize the 6-carbon citric acid back into a 4-carbon oxaloacetic acid and two carbon dioxide molecules. At the same time three NAD^+ and one FAD are reduced into three NADH and one $FADH_2$ respectively, and one ATP is produced by substrate level phosphorylation. (Recall, 1 glucose $\longrightarrow$ 2 pyruvate acid $\longrightarrow$ 2aceytl, so this cycle runs twice) (Hickman et al., 1997) The net equation for citric acid cycle is

$$\begin{aligned} 2AcetylCoA \quad + \quad & 6NAD^+ + 2FAD + 2ADP + 2Pi + 4H_2O \\ & \longrightarrow 2CoA + 6NADH + 2FADH_2 + 2ATP + 4CO_2 + 4H^+. \end{aligned}$$

Oxidative phosphorylation occurs on a membrane, the mitochondrial cristae. It includes the Electron Transport Chain(ETC)and ATP synthesis. The final stage of Oxidative phosphorylation generates most of the ATP produced from glucose. Co-enzymes from the previous reactions pass electrons to a series of electron carrier molecules, which carry out redox reactions resulting in the chemosmotic generation of ATP (McMurry et al., 1996; Hickman et al., 1997). The net equation for oxidative phosphorylation is

$$2NADH(from\, glycolysis) + 2NADH(from\, Decarboxylation) +$$

$$+6NADH(from\, Citric\, Acid\, Cycle) + 2FADH_2(from\ citric\ Acid\ Cycle) +$$

$$+6O_2 + 32ADP + 32Pi \longrightarrow 12H_2O + 32ATP + 10NAD^+ + 2FAD.$$

The net ATP yield per glucose molecules from complete oxidation of 1 glucose molecule is 30-32 ATP. In general, most eukaryotic cells produces about 36 ATP molecules during aerobic respiration. The net equation for aerobic respiration which yied most of the energy in form of ATP is

$$C_6H_{12}O_6 + 6O_2 + 36ADP + 36P \longrightarrow 6CO_2 + 6H_2O + 36ATP.$$

The model discussed here tries to describe the change in the volume of ATP, the concentration of glucose (sugar) and the actual energy release in the cell. Detailed studies on the synthesis

of ATP in the mitochondria can be found in Ejikeme (2006); Harris & Das (1991); Korla and Mitra (2014).

In Korzeniewski (1996), introduced a mathematical dynamic model of oxidative phosphorylation in isolated hepatocytes incubated with different respiratory substrates. The model showed the energetic behaviour of the cell during great variations of the respiration rate and proton-motive force. Computer simulated models of oxidative phosphorylation and Krebs cycle also been introduced (Korzeniewski, 1998; Korla and Mitra, 2014).

In Ayeni et al. (2005) introduced a model of the energy generation in a combustion engine, in their model they showed that even in a non-homogeneous reaction, the critical Frank-Kemenetskii parameter increases as the radiation parameter increases when the activation energy is high. The combustion equations for their models are:

$$P_g \frac{\partial T_g}{\partial t} = \lambda_g \frac{\partial^2 T_g}{\partial x^2} + C_f Q_f \alpha_g A e^{\frac{-E}{R} T_g} - 4\pi R_d n_d (T_g - T_0) - 4\pi R_d^2 \alpha_1 n_d (T_g^4 - T_0^4), \quad (1)$$

$$\frac{d(R_d^2)}{dt} = -\frac{2\lambda_g}{\rho L}(T_g - T_0) - \frac{4\pi R_d \sigma}{L\rho}(T_g^4 - T_0^4), \quad (2)$$

$$\alpha_g \frac{\partial C_f}{\partial t} = D_f \frac{\partial^2 C_f}{\partial x^2} - C_f \alpha_g \mu_f A e^{-\frac{E}{R} T_g} + \frac{4\pi R_d \lambda_g n_d (T_g - T_0)}{L \mu_g \alpha_g} + \frac{4\pi R_d^2 \sigma_1 n_d (T_g^4 - T_0^4)}{L \mu_g \alpha_g}, \quad (3)$$

where together with initial and boundary conditions

$$T_g(x,0) = T_0, \quad C_f(x,0) = C_{f_0}, \quad R_d(0) = R_{d_0}.$$

$$T_g(-1,t) = T_g(1,t) = T, C_f(-1,t) = C_{f_{-1}}, C_f(1,t) = C_{f_1},$$

where T represents Temperature, E is activation energy of the system, L is the liquid evaporation energy, C is the concentration of reactant. R_d stands for the radius of drop, Q is heat released per unit mass, P_g is the constant of proportionality, $\alpha_1 = \frac{2\alpha\varepsilon_d}{2-\varepsilon_d}$, α is Stefan-Bottzman constant, ε_d is emissivity of the droplets on surface, μ is the molar mass of reactant, ρ is density, α_g is volumetric phase constant, n is the number of drops per unit volume λ is thermal conductivity, A is pre-exponential factor, R is the universal gas constant. The subscripts: g represent gas mixture f represents combustible gas component of the mixture while d is the liquid drops. Details on the formulation of equations (1) - (3) can be found in the paper (Ayeni et al., 2005).

In Ejikeme et al. (2011), adapted and modified the model of the energy generation in a combustion engine introduced by Ayeni et al. (2005) to produced a model for the energy generation in the mitochondria of the human cell. This was done by comparing the detailed functioning of a diesel engine with what happens in the human body or system. Comparing these two process of energy generation in two different system, they observed some similarities between the two systems. Motivated by their work, we reformulated their model using fractional derivatives in the sense of Caputo.

2 The Mathematical Model of Energy Generation in Human Body by Human Cell

In this section we discuss the derivation of the mathematical model of energy generation in the mitochondria of human cell as presented and by Ejikeme et al. (2011). We first discussed the derivation of the integer derivative model and introduced the fractional derivative analogue of the model. We adopted the Caputo fractional derivative in the fractional model.

2.1 The Integer Derivative model

The living body is a chemical engine and because it is an engine it must like diesel engine (or engine of a motor car) be constantly supplied with diesel (or fuel) to keep it working. Such diesel

needs to be provided by the food we eat, and when it is supplied to the body it is "Com-busted" with the oxygen of the air we breathe. The result of this "Combustion" is the release of the necessary energy to keep the body alive. This implies that a comparatively good description of what happens in the human system is the process of energy generation in a diesel engine which generates the energy that sustains the running of the engine. The diesel engine has a carburetor (equivalent to the mitochondria) where the diesel is ignited and burnt to release heat energy. Just like the reaction in the Kreb's Cycle or Citric Acid cycle and Mitochondria, Oxygen is very important since we also know that there would be no combustion in the absence of oxygen. The detailed functioning of a diesel engine is compared here with what happens in the human body. Comparing these two process of energy generation in two different system, it is found that they are alike in many ways.

The detailed functioning of a diesel engine is compared here with what happens in the human body or system. Comparing these two process of energy generation in two different system, it is found that they are alike in many ways. The energy sources are similar-hydrocarbon. The initial source of energy to enable subsequent energy generation that sustains the systems was provided by the glycolytic pathway and the battery respectively. The burning of the sources of energy (glucose and fuel or diesel) is provided with chambers (mitochondria and carburetor) that are highly regulated. This is seen by comparing the inflow of glucose (in the form of accetyl CoA) into the mitochondria which is regulated by the fuel droplets into the carburetor which on its own is regulated by the metering processes. Based on these similarities in the two systems on their energy generation processes and requirements, the combustion in the carburetor can be liken to ATP production in the mitochondria. In their paper, Ejikeme et al. (2011), (see also (Ejikeme, 2006)), adopted and adapted the models describing the non-homogeneous combustion reaction in the carburetor to the energy generation in the mitochondria with proper modifications to take care of the nature of the systems (the human cells) involved in the reactions.

Since not much heat is released ordinarily in the human system, the interest is particularly about equation (2) and (3). These equations are modified to truly reflect and or represent the system being studied. From biological studies, glycolysis occurs at physiologically constant temperature which is 37^0 C. Thus, our term $T_g - T_0$ can simply be represented by T. Also the activation energy can be taken as a constant since glycolysis is a spontaneous process and does not require any extra energy order than that present at the initial time. The process generates subsequent energy it needs to continue the process. Thus, the activation energy in this work will then be taken as the energy supplied by the glycolytic pathway which is the 2ATP and as such E is constant per mole of glucose. Since the process occurs in the cell and considering the nature of the cell, evaporation does not occur so that the liquid evaporation energy is constant if at all it is required. The reactants in our study here are the sugar (glucose) and oxygen. The radius of drop can be similarly taken here to mean the volume of the glucose that enters into reaction which can be measured in mole, thus R_d in equations (2) and (3) is replaced with V.

In the human cell, the thermal conductivity is considered such that its value is zero, although it is known that excess heat is removed from the body by perspiration or sweating but no external heat is added. The subscripts appearing in the terms of equations (2) and (3) are neglected since sugar(glucose) does not appear in gaseous forms. With the above modification on equations (2) and (3), we arrive at the following equations

$$\frac{d(V^2)}{dt} = -\frac{4\pi V\sigma_1 T^4}{G\rho}, \tag{4}$$

$$\nu\frac{\partial C}{\partial t} = D\frac{\partial^2 C}{\partial x^2} - C\nu\mu\Lambda e^{-\frac{E}{\mu}T} + \frac{4\pi V^2\sigma_1 m T^4}{G\mu\nu}, \tag{5}$$

where $V = V(t)$, $\quad C = C(x,t)$, together with initial and boundary conditions

$$V(0) = V_0(\text{constant}),$$
$$C(x,t) = C_i, \quad \text{at} x = \pm i, \ i = 1,$$

where V is the volume of glucose that enters into the mitochondria in the oxidized form and C_i is the concentration of reactants at positions $x = \pm 1$. Equations (4) and (5) represent the model for energy generation in the mitochondria of human cell which were first formulated and studied by (Ejikeme et al., 2011).

In the current paper, we reformulated the model using fractional derivatives in the sense of Caputo. We first considered the integer derivative model. For the purpose of the method we are to use in solving this problem we assume that the boundary are at a position $x = 0$ and $x = 1$. We also assume that the concentration of reactants at the boundaries $C(0,t) = 0$ and $C(1,t) = c_0$ (constant). Let $\Omega = [0,1] \times [0,2]$, we considered the following model

$$\frac{d(V^2)}{dt} = -\frac{4\pi V \sigma_1 T^4}{G\rho}, \quad t \in [0,2], \tag{6}$$

$$\nu \frac{\partial C}{\partial t} = D\frac{\partial^2 C}{\partial x^2} - C\nu\mu\Lambda e^{-\frac{E}{RT}} + \frac{4\pi V^2 \sigma_1 m T^4}{G\mu\nu}, \quad (x,t) \in \Omega, \tag{7}$$

where $V = V(t), \quad C = C(x,t)$, together with initial and boundary conditions

$$\begin{aligned} &V(0) = V_0(\text{constant}), \\ &C(0,t) = 0, \quad \text{and} \quad C(1,t) = c_0, \quad t \in [0,2], \end{aligned} \tag{8}$$

where V is still the volume of glucose that enters into the mitochondria in the oxidized form as ATP and c_0 is the concentration of reactants at the boundaries.

In the model above, V_0 is the initial volume of glucose in the mitochondria in oxidized form as ATP, c_0 is concentration of reactants at the boundary of the membrane at any time. The reaction that leads to the generation of ATP takes place in the inner membrane of the mitochondria. From biological point of view, glycolysis occurs at physiologically constant temperature which is $37°C$. Thus T which denote temperature is constant. The parameter $\sigma_1 = \frac{2\sigma\varepsilon}{2-\varepsilon}$, where σ is the Stefan-Boltzmann constant and ε is the dissociation constant, G is dissociation energy of the glucose molecules(this is the energy needed to break every chemical bond in glucose molecule and completely separate all its atoms; the SI units used to describe bond energy are (kJ/mol)). The number of glucose per unit volume is denoted by m. The volumetric phase constant is denote by ν, this tells how much a signal is shifted along the x-axis; for example, a phase constant of Q means that each value of the signal happens Q amount of the time earlier. In Chemistry and physics, activation energy is the energy which must be available to a chemical or nuclear system with potential reactants to result in a chemical reaction , nuclear reaction or various other physical phenomena. It is defined as a least possible (minimum) amount of energy which is required to start a reaction or the amount of energy available in a chemical system for a reaction to take place. The activation energy in the form of ATP is denoted by E. Λ represent the pre-exponential(or frequency) factor. The pre-exponential factor or constant in the Arrhenius equation $k = \Lambda e^{-\frac{E}{RT}}$ is an empirical relationship between temperature and rate coefficient, k. R denotes the universal gas constant. The quantity μ represent the molar mass of hydrocarbon, C is concentration of the reactant, D is diffusion coefficient and ρ denotes the density of glucose, $\rho = \frac{\nu}{V}$.

These equations represent the system being studied. The temperature T is taking to be a constant. Also the activation energy can be taken as a constant since glycolysis is a spontaneous process and does not require any extra energy order than that present at the initial time. The process generates subsequent energy it needs to continue the process. Thus, the activation energy in this work will then be taken as the energy supplied by the glycolytic pathway which is the 2ATP and as such E is constant per mole of glucose. Since the process occurs in the cell and considering the nature of the cell, evaporation does not occur so that the liquid evaporation energy is constant if at all it is required. The reactants in our study here are the sugar (glucose)

and oxygen. In the human cell, it is known that excess heat is removed from the body by perspiration or sweating but no external heat is added.

We remark that the two equations (4) and (5) describe the change in the volume of the reactants that enters the mitochondria in the oxidized forms over a period of time as well as the change in the concentration of reactants over a period of time. It is this change in the concentration of reactants that produces the energy which is transported in the form ATP to places where they are needed in the human body. In addition, equation (5) also describe the diffusion of reactants within the inner membrane of the mitochondria. For simplicity, we re-write equation (5) as

$$\frac{\partial C}{\partial t} - \frac{D}{\nu}\frac{\partial^2 C}{\partial x^2} + \mu\Lambda e^{-\frac{E}{RT}}C - \frac{4\pi\sigma_1 m T^4}{G\mu\nu^2}V^2 = 0, \quad (x,t) \in \Omega$$

which simplifies to

$$\frac{\partial C}{\partial t} - k_1\frac{\partial^2 C}{\partial x^2} + k_2 C - k_3 V^2 = 0, \quad (x,t) \in \Omega, \tag{9}$$

where $k_1 = \frac{D}{\nu}$, $k_2 = \mu\Lambda e^{-\frac{E}{RT}}$ and $k_3 = \frac{4\pi\sigma_1 m T^4}{G\mu\nu^2}$.
Solving (4) and applying the initial conditions, we get

$$V_0 - V = \frac{2\pi\sigma_1 T^4}{G\rho}t. \tag{10}$$

This implies that $V_0 > V$ has a valid result at $t > 0$. Thus we have that

$$V = V_0 - \frac{2\pi\sigma_1 T^4}{G\rho}t = V_0 - k_4 t, \quad \text{where } k_4 = \frac{2\pi\sigma_1 T^4}{G\rho}. \tag{11}$$

Substituting equation (11) into (9) we get

$$\frac{\partial C}{\partial t} - k_1\frac{\partial^2 C}{\partial x^2} + k_2 C - k_3(V_0 - k_4 t)^2 = 0. \tag{12}$$

Thus the required model describing the unsteady state non-homogeneous combustion reaction in human body is simplified to

$$\frac{\partial C}{\partial t} - k_1\frac{\partial^2 C}{\partial x^2} + k_2 C - k_3(V_0 - k_4 t)^2 = 0, \tag{13}$$

subject to the boundary condition

$$C(0,t) = 0, \quad C(1,t) = C_0. \tag{14}$$

At the steady state,

$$\frac{\partial C}{\partial t} = 0 \text{ and } V^2(t) = V_0 \ (say),$$

the volume of glucose remain constant so that equation (13) becomes,

$$k_1\frac{\partial^2 C}{\partial x^2} - k_2 C + k_3 V_0 = 0. \tag{15}$$

2.2 The Fractional Derivative Model

All of the models discussed above involve ordinary differential equations with integer order derivatives. In this paper, the model of energy generation in the mitochondria is reformulated using fractional order derivatives. That is, we consider the equation (13) where the integer time and space derivatives involve in the equation are replaced with Caputo type fractional-time and -space derivatives. The fractional model of energy generation in a human cell studied in this paper is given as

$$\frac{\partial^\alpha C}{\partial t^\alpha} - k_1 \frac{\partial^2 C}{\partial x^2} + k_2 C - k_3 (V_0 - k_4 t)^2 = 0, \quad (x,t) \in \Omega, \tag{16}$$

subject to the boundary condition

$$C(0,t) = 0, \quad C(1,t) = c_0, \tag{17}$$

where $0 < \alpha \leq 1$.

By introducing fractional-time derivative, some characteristic behaviour of the system not captured by the integer case model may be captured in this fractional-time derivative model. Besides, some measure of chaoticness (if any) that may occur in the process of energy generation may be seen in the fractional-time derivative model. The behaviour of the system as $\alpha \longrightarrow 1$ will be examined and compared with the integer derivatives.

For the fractional-time derivative model, the case $\frac{\partial^\alpha C}{\partial t^\alpha} = 0$ corresponds to the steady state integer derivative model. However, we are interested in the case where $\frac{\partial^\alpha C}{\partial t^\alpha} \neq 0$. This is a non-homogeneous fractional-time differential equation whose solution is to be obtained using Homotopy Analysis Method (HAM).

3 Introduction to Fractional Calculus

In this section, we recall some of the definitions and results needed from fractional differential and integral calculus. For more details, the reader can refer to Diethelm & Ford (2002); Poblubny (1999).

Definition 1. *(Diethelm & Ford, 2002) Let $n \in \mathbb{R}_+$. The operator J_a^n, defined on $L_1[a,b]$ by*

$$J_a^n f(x) := \frac{1}{\Gamma(n)} \int_a^x (x-t)^{n-1} f(t) dt$$

for $a \leq x \leq b$, is called the Riemann- Liouville fractional integral operator of order n. For $n = 0$, we set $J_a^0 := I$, the identity operator.

Definition 2. *(Diethelm & Ford, 2002) Let $n \in \mathbb{R}_+$ and $m = [n]$. The operator D_a^n, defined by*

$$D_a^n f := D^m J_a^{m-n} f$$

is called the Riemann- Liouville fractional differential operator of order n. For $n = 0$, we set $D_a^0 := I$, the identity operator.

Theorem 1. *(Diethelm & Ford, 2002) Let $n \geq 0$. Then, for every $f \in L_1[a,b]$,*

$$D_a^n J_a^n f = f,$$

almost everywhere.

Lemma 1. *(Diethelm & Ford, 2002) Let $n \geq 0$ and $m = [n]$. Assume that f is such that both $D^n_{*a} f$ and $D^n_a f$ exist. Then,*

$$D^n_{*a} f(x) = D^n_a f(x) - \sum_{k=0}^{m-1} \frac{D^k f(a)}{\Gamma(k-n+1)} (x-a)^{k-n},$$

where the operator D^n_{*a} defined by

$$D^n_{*a} f := D^n_a [f - T_{m-1}[f; a]]$$

is called the Caputo differential operator of order n.

Theorem 2. *(Diethelm & Ford, 2002) Assume that $n \geq 0$, $m = [n]$ and $f \in A^m[a, b]$. Then,*

$$J^n_a D^n_{*a} f(x) = f(x) - \sum_{k=0}^{m-1} \frac{D^k f(a)}{k!} (x-a)^k,$$

where $A^m[a, b]$ is the set of functions with absolutely continuous derivative of order $m - 1$.

4 Homotopy Analysis Method for Differential Equations

The homotopy analysis method (HAM) is an analytical approximation method for solving linear and nonlinear ordinary and partial differential equations. It uses the concept of the homotopy from topology to generate a convergent series solution using the homotopy-Maclaurin series to resolve the nonlinearities in the equation. This method was first introduced by Liao (1992) and been used by many authors to solve many types of problems in Science and engineering (Abbasbandy, 2006; Song & Zhang, 2007; Hetmaniok et al., 2014). The method may be used to obtain the exact solution or a power series solution which converges, in general, to exact solution. The HAM consists of parameter $\hbar \neq 0$ which is called the convergence control parameter. This parameter controls the convergent region and rate of convergence of the series solution (Chakraverty et al., 2019).

The novelty of the HAM lies in the fact that it does not depend on small or large physical parameters. Thus, it is applicable to problems with strong nonlinearity. Most traditional perturbation methods are based on small parameter assumption. However, many nonlinear problems have no small parameters at all. Besides, the determination of small parameters is a special techniques. Moreover, these small parameters are so sensitive, in the sense that a small change in small parameters will affect the results. An appropriate choice of small parameters leads to ideal results while an unsuitable choice of small parameters may results in bad effects (Chakraverty et al., 2019). Thus, a method that could bypass the small parameter assumption is deemed a better method. The HAM also distinguishes itself in that it is a unified method for the Lyapunov artificial small parameter method, the delta expansion method, the Adomian decomposition method, Adomian & Adomian (1984) and the homotopy perturbation method (Liang & Jeffrey, 2009; Sajid & Hayat, 2008). The greater generality of the method often allows for strong convergence of the solution over larger spatial and parameter domains. It also gives an excellent flexibility in the expression of the solution and how the solution is explicitly obtained. It provides great freedom to choose the basis functions of the desired solution and the corresponding auxiliary linear operator of the homotopy. Finally, unlike the other analytic approximation techniques, the HAM provides a simple way to ensure the convergence of the solution series.

To illustrate the procedure of applying HAM, we consider the following nonlinear differential equation

$$N[u(t)] = 0, \tag{18}$$

where N is a nonlinear operator, t denotes the independent variable and u is an unknown function. By means of HAM, we can construct the zeroth-order deformation equation

$$(1-q)L[\phi(t:q)-u_0(t)] = q\hbar H(t)N[\phi(t:q)], \tag{19}$$

where $q \in [0,1]$ is the embedding parameter, $\hbar \neq 0$ is an auxiliary parameter and $H(t)$ denotes a non-zero auxiliary functions. L, an auxiliary linear operator which possesses the property $L(C) = 0$, $u_0(t)$ is the initial guess of $u(t)$, $\phi(t,q)$ is a function of the homotopy parameter $q \in [0,1]$. When the embedding parameter $q = 0$ and $q = 1$ equation (19) becomes

$$\phi(t:0) = u_0(t), \quad \phi(t:1) = u(t), \tag{20}$$

respectively. Thus as q increases from 0 to 1, the solution varies from the initial guess $u_0(t)$ to the solution $u(t)$. This kind of variation is called deformation. For equation (18), one constructs the homotopy equation involving $\phi(t:q)$ (19) which is called the zero-order deformation equation.

With the freedom of choosing the auxiliary parameter $\hbar$, the auxiliary function $H(t)$, the initial approximation $u_o(t)$ and the auxiliary linear operator L, we can assume that all of them are properly chosen so that the solution $\phi(t:q)$ of the zeroth-order deformation equation exists for $0 \leq q \leq 1$.

Expanding $\phi(t:q)$ in Taylor series with respect to q, we have

$$\phi(t:q) = u_0(t) + \sum_{m=1}^{\infty} u_m(t)q^m, \tag{21}$$

where

$$u_m(t) = \frac{1}{m!}\frac{\partial^m \phi(t:q)}{\partial q^m}|_{q=0}. \tag{22}$$

The convergence of equation (21) depends upon the auxiliary parameter $\hbar$. If it is convergent, then at $q = 1$, we have

$$u(t:1) = u_0(t) + \sum_{m=1}^{\infty} u_m(t)$$

which must be one of the solutions of the original nonlinear equation as proved by (Liao & Tan, 2007). When $\hbar = -1$ and $H(t) = 1$, (19) becomes

$$(1-q)L[\phi(t:q)-u_0(t)] + qN[\phi(t:q)] = 0. \tag{23}$$

The governing equation and the corresponding initial condition of $u_m(t)$ can be deduced from the zero-order deformation equation (19). Indeed, if one defines the vectors

$$\bar{u}_n = \{u_0(t), u_1(t), \cdots, u_m(t)\}$$

and differentiate the zeroth-order deformation equation (19) m times with respect to q setting $q = 0$ and then dividing them by $m!$ we get the so-called $mth-$ order deformation equation given as

$$L[u_m(t) - \chi_m u_{m-1}(t)] = \hbar H(t) R_m(\bar{u}_{m-1}), \tag{24}$$

where

$$R_m(\bar{u}_{m-1}) = \frac{1}{m!}\frac{\partial^{m-1} N[\phi(t:q)]}{\partial q^{m-1}}|_{q=0} \tag{25}$$

and

$$\chi_m = \begin{cases} 0, m \leq 1 \\ 1, m > 1. \end{cases} \tag{26}$$

We remark that since $u_m(t)$ for $m \geq 1$ is governed by the linear equation (24) with linear boundary conditions that comes from the original problem, one can obtain its solution $u_m(t)$, by the means of some symbolic computation software such as Mathematica, Maple and Matlab.

5 Homotopy Analysis method (HAM) for integer case model of Energy generation in human body

In this section, we obtain the solution to the integer model of energy generation in mitochondria, equations (6) - (8), using the Homotopy Analysis Method (HAM). In particular, we solve the following boundary value problem of unsteady state model of energy generation in the mitochondria of human cell using HAM.

$$\begin{cases} \frac{\partial C}{\partial t} - k_1 \frac{\partial^2 C}{\partial x^2} + k_2 C - k_3 (V_0 - k_4 t)^2 = 0, \quad (x,t) \in \Omega, \\ C(0,t) = 0, \quad C(1,t) = c_0. \end{cases} \tag{27}$$

Following the Homotopy Analysis method, we choose the take the linear operator to be

$$L[\phi(x,t;q)] = \frac{\partial^2 \phi}{\partial x^2},$$

which satisfies the condition that

$$L[k_1 + k_2 x] = 0.$$

The inverse operator is defined as

$$L^{-1} = \int_0^x \int_0^s d\tau ds.$$

The zeroth order deformation equation is given as

$$(1-q)L[\phi(x,t;q) - \phi_0(x,t;q)] = q\hbar H(x,t) N[\phi(x,t;q)], \tag{28}$$

subject to

$$\phi(0,t) = 0 \quad \text{and} \quad \phi(1,t) = C_0,$$

where $q \in [0,1]$ and $\phi_0(x,t;q)$ is the initial guess function. The operator $N[\phi(x,t;q)]$ is given as

$$N = \frac{\partial \phi}{\partial t} - k_1 \frac{\partial^2 \phi}{\partial x^2} + k_2 \phi - k_3 (V_0 - k_4 t)^2.$$

We remark that when $q = 0$, the zeroth order deformation equation leads to

$$\phi(x,t;0) = \phi_0(x,t;0),$$

and when $q = 1$, it leads to

$$N = \frac{\partial \phi}{\partial t} - k_1 \frac{\partial^2 \phi}{\partial x^2} + k_2 \phi - k_3 (V_0 - k_4 t)^2 = 0.$$

This implies that

$$\phi(x,t;0) = \phi_0(x,t)$$

and

$$\phi(x,t;1) = C(x,t)$$

which is the solution to the equation

$$N[\phi(x,t;1)] = 0.$$

The Taylor series expansion of the function $\phi(x,t;q)$ with respect to the embedding parameter is gives as

$$\phi(x,t;q) = \phi_0(x,t) + \sum_{m=1}^{\infty} C_m(x,t) q^m, \tag{29}$$

where $C_m(x,t) = \frac{1}{m!}\frac{\partial^m \phi(x,t;q)}{\partial q^m}\Big|_{q=0}$.

According to Homotopy Analysis Method, when the linear operator L, the initial approximation function, $\phi_0(x,t)$, the auxiliary parameter $\hbar$ and the auxiliary function, $H(x,t)$ are chosen correctly, the series (29) converge for $q = 1$. So that,

$$\phi(x,t;1) = \phi_0(x,t) + \sum_{m=1}^{\infty} C_m(x,t), \tag{30}$$

which implies that

$$C(x,t) = \phi_0(x,t) + \sum_{m=1}^{\infty} C_m(x,t)$$

which will be the solution to the original equation with an appropriate guess function phi_0.

The solution $C(x,t)$ can be obtained from the so called m^{th} order deformation equation which is given as

$$L[C_m(x,t) - \chi_m C_{m-1}(x,t)] = \hbar H(x,t) R_m(C_{m-1}(x,t)), \qquad m \geq 1, \tag{31}$$

subject to

$$C_m(0,t) = C_m(1,t) = 0, \tag{32}$$

where

$$\chi_m = \begin{cases} 0, & \text{if } m \leq 1 \\ 1, & \text{if } m > 1 \end{cases}$$

and

$$\begin{aligned} R_m(C_{m-1}) &= \frac{1}{(m-1)!}\frac{\partial^{m-1}}{\partial q^{m-1}} N[\phi(x,t;q)]\Big|_{q=0} \\ &= \frac{\partial}{\partial t}C_{m-1} - k_1\frac{\partial^2}{\partial x^2}C_{m-1} + k_2 C_{m-1} - (1-\chi_m)k_3(V_0 - k_4 t)^2. \end{aligned}$$

Following the procedure of HAM, we chose the auxiliary function $H(x,t) = 1$, the initial guess function $phi_0(x,t) = c_0$ and apply the inverse operator, L^{-1}, on the mth order deformation equation to get

$$\begin{aligned} C_m(x,t) &= \chi_m C_{m-1}(x,t) + \hbar L^{-1}\left[R_m(C_{m-1}(x,t))\right] \\ &= \chi_m C_{m-1}(x,t) \\ &\quad + \hbar \int_0^x \int_0^s \left[\frac{\partial}{\partial t}C_{m-1} - k_1\frac{\partial^2}{\partial x^2}C_{m-1} + k_2 C_{m-1} - (1-\chi_m)k_3(V_0 - k_4 t)^2\right] d\tau ds \\ &\qquad + c_1 + c_2 x, \end{aligned} \tag{33}$$

where c_1 c_2 are constants to be determined.

Applying the initial conditions (32), we get

$$\begin{aligned} c_1 &= -\chi_m C_{m-1}(0,t) \quad \text{and} \\ c_2 &= \chi_m C_{m-1}(0,t) \\ &\quad - \hbar \int_0^1 \int_0^s \left[\frac{\partial}{\partial t}C_{m-1} - k_1\frac{\partial^2}{\partial x^2}C_{m-1} + k_2 C_{m-1} - (1-\chi_m)k_3(V_0 - k_4 t)^2\right] d\tau ds \\ &\qquad - \chi_m C_{m-1}(1,t), \end{aligned}$$

so that the solution of the mth order deformation equation becomes

$$\begin{aligned} C_m(x,t) &= \chi_m C_{m-1}(x,t) \\ &+\hbar \int_0^x \int_0^s \left[\frac{\partial}{\partial t} C_{m-1} - k_1 \frac{\partial^2}{\partial x^2} C_{m-1} + k_2 C_{m-1} - (1-\chi_m) k_3 (V_0 - k_4 t)^2 \right] d\tau ds \\ &-\chi_m C_{m-1}(0,t) + [\chi_m C_{m-1}(0,t) - \chi_m C_{m-1}(1,t)]\, x \\ &-\hbar x \int_0^1 \int_0^s \left[\frac{\partial}{\partial t} C_{m-1} - k_1 \frac{\partial^2}{\partial x^2} C_{m-1} + k_2 C_{m-1} - (1-\chi_m) k_3 (V_0 - k_4 t)^2 \right] d\tau ds \end{aligned} \tag{34}$$

Thus the solution to the original equation (27) is

$$\begin{aligned} C(x,t) &= \phi_0(x,t) + \sum_{m=1}^{\infty} C_m(x,t) \\ &= c_0 + \sum_{m=1}^{\infty} C_m(x,t). \end{aligned} \tag{35}$$

6 Convergence of HAM solution

In this section, the convergence of the HAM solution in (35) for order m = 5, is discussed. The convergence of the HAM solution depend on the control parameter $\hbar$. In this regard we plot $\hbar$-curve with appropriate values assigned to the constants and parameters associated with the model.

Values of Parameters of the model for numerical computations

In order to display the results graphically, a few reasonable assumptions were made regarding the values of data used in plotting the graphs. However, some of the data were calculated using standard equations as obtained from experimental results found in the literature.

For the purpose of this study, the rate constants for all reactions has been assumed to be 1 (i.e. k =1), since rate constants varies depending on the temperature and other experimental conditions. The dissociation constant,ε, for glucose is obtained experimentally and it varies according to the complexities in the reaction. Thus we assumed a value of 0.069mM for the purpose of this research. The density of glucose is known to be $1.56g/cm^3$ while the volume of glucose that enters the mitochondria V is assumed to be $4.375\times10^{-8}cm^3$, so that the volumetric phase constant $\nu = \rho V = 6.28 \times 10^{-8}$. The number of glucose per unit volume, m, is assume to be 2. The universal gas constant is given as 8.314472J/mol K. The temperature is take to be $37°C(310.15K)$. The Pre-exponential factor Λ is a factor that is determined experimentally, as it varies with different reactions, thus we assume it to be 2. The molar mass of hydrocarbon $\mu = n(C) * 12.010107 + n(H) * 1.00794$ where $n(C)$ is the number of carbon atoms in the hydrocarbon molecule and $n(H)$ is the number of hydrogen in the hydrocarbon molecule. Thus the molar mass of hydrocarbon μ is taken to be 84.1559224. The activation energy $E \approx 1787.44J$ which is calculated using the Arrhenius equation $k = \Lambda e^{-\frac{E}{RT}}$, where k is the rate constant, A is the pre-exponential factor, correlating with the number of properly-oriented collisions, E is the activation energy, R is the universal gas constant and T is the temperature in Kelvin. Dissociation energy of Glucose, G(The energy needed to break all chemical bonds in Glucose)is obtained from the bond energy of each bound type associated with glucose. The table below (figure 1) shows the figures for the various bond type.

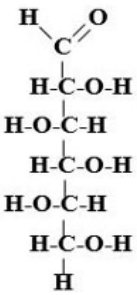

Bond Type	Quantity	Bond Energy (kJ/mol)	Total Bond Energy
C-C	5	347	1735
O-H	5	464	2320
C-H	7	414	2898
C-O	5	358	1790
C=O	1	803	803
		Total Bond Energy for Glucose	9546kJ/mol

Figure 1: Bounding Molecules and Bound Energies for glucose

The $\hbar$-curves

The $\hbar$-curves for different values of the coefficient of diffusion term, at 5th order approximation and at $x = 0.2, \quad t = 2$ is shown in figure 2. According to (Liao, 2003) see also (Mastroberardino, 2011), the interval of convergence is determined by the flat portion of the $\hbar$-curve. From Figure 2 the admissible interval of convergence that is common to all the curves considered is $[-1, 0) \cup (0, 1]$.

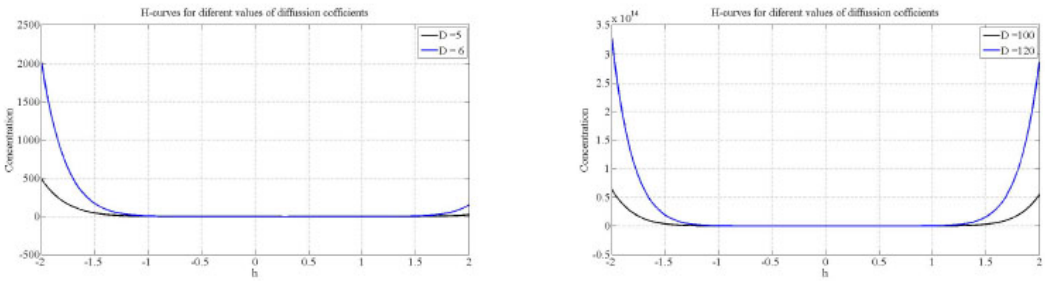

(a) $D = 5, \quad D = 6$ (b) $D = 100, \quad D = 120$

Figure 2: $\hbar$ - Curves for different values of D at $x = 0.2$ $t = 2$

7 Numerical Example and Surface plots of HAM solution

In order to practically illustrate the method discussed above, we consider the following example:

$$\begin{cases} \frac{\partial C}{\partial t} - k_1 \frac{\partial^2 C}{\partial x^2} + k_2 C - k_3(2 - k_4 t)^2 = 0, \quad (x,t) \in \Omega \\ C(0,t) = 0, \quad C(1,t) = 2, \end{cases} \tag{36}$$

where, in particular, we take $(k_1, k_2, k_3, k_4) = (0.3205, 157.1896, 0.000482, 0.0158)$. We obtain an approximate HAM solution, sketch it surface plot and compute its error function.

Following HAM technique, we choose the auxiliary control parameter $\hbar = -1$ and the diffusion coefficient $D = \frac{1}{2}$, so the solution to the BVP (36) is given as follows:

$$\begin{aligned} C_1(x,t) &= (0.000241(0.0158t - 2.0)^2 - 157.0)x^2 - (0.000241(0.0158t - 2.0)^2 - 157.0)x. \\ C_2(x,t) &= 1.32x^2(0.000241(0.0158t - 2.0)^2 - 157.0) - x(0.0000000101t + 0.00323(0.0158t - 2.0)^2 - 2111.0) \\ &\quad -x(2.41e - 4(0.0158t - 2.0)^2 - 157.0) - 1.0x^4(1.01e - 8t + 0.00316(0.0158t - 2.0)^2 - 2066.0) \\ &\quad +1.0x^3(2.01e - 8t + 0.00631(0.0158t - 2.0)^2 - 4122.0) \cdots \end{aligned}$$

These approximate solutions were obtained using the symbolic tool of MATLAB. More solution were obtained and used in plotting the graphs. The solution of the BVP, up to order N, is therefore gives as

$$C_N(x,t) = C_1 + C_2 + C_3 + \cdots + C_N = \sum_{i=1}^{N} C_1(x,t). \tag{37}$$

This is given as

$$\begin{aligned} C_N(x,t) \quad = \quad & 0.75x^4(-0.00000519t^2 + 0.00131t + 13500) - 0.5x^6(-0.0000248t^2 + 0.00628t + 64700) \\ & -x^2(-0.0000203t^2x^8 + 0.000101t^2x^7 + 0.0000498t^2x^6 - 0.000808t^2x^5 - 0.0000269t^2x^4 \\ & +0.00334t^2x^3 + 0.00000314t^2x^2 - 0.00671t^2x - 0.000000445t^2 + 0.00513tx^8 - 0.0257tx^7 \\ & -0.0126tx^6 + 0.204tx^5 + 0.0068tx^4 - 0.843tx^3 - 0.000795tx^2 + 1.7tx + 0.0000113t \\ & +52900x^8 - 264000x^7 - 130000x^6 + 2110000x^5 + 70100x^4 - 8690000x^3 - 8199.0x^2 \\ & +17500000x + 116.0) - 5.0x(0.000241(0.0158t - 2.0)^2 - 157.0) \\ & -4.0x(0.0000000101t + 0.00323(0.0158t - 2.0)^2 - 2111.0) \cdots \end{aligned}$$

The surface plot of the solution by HAM at different values of $\hbar$ and D are shown in figures 3 and 4.

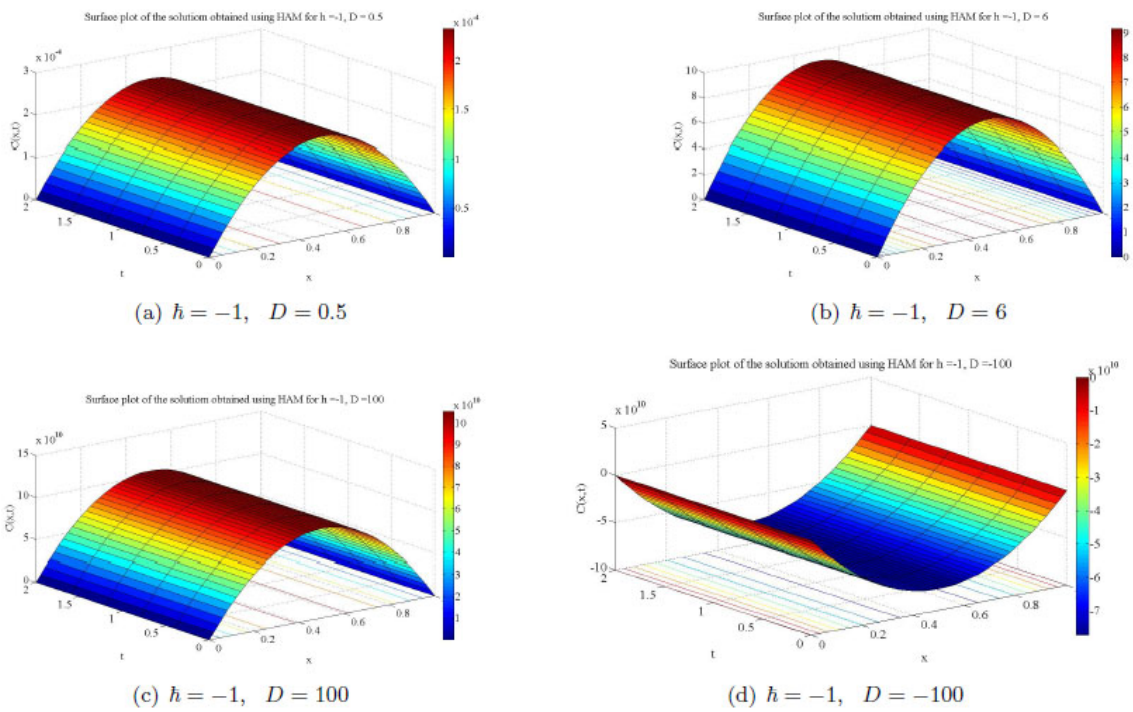

(a) $\hbar = -1, \quad D = 0.5$ (b) $\hbar = -1, \quad D = 6$

(c) $\hbar = -1, \quad D = 100$ (d) $\hbar = -1, \quad D = -100$

Figure 3: Surface plots of HAM solution for $\hbar = -1$ and different values of diffusion coefficient, D

This figure shows that the energy generated in the human cell increases with time to a maximum value when the rate of diffusion (a measure of usage by the cell) is positive and then begins to decreases as it is being used to do work. When the rate of diffusion is negative then no energy is produced.

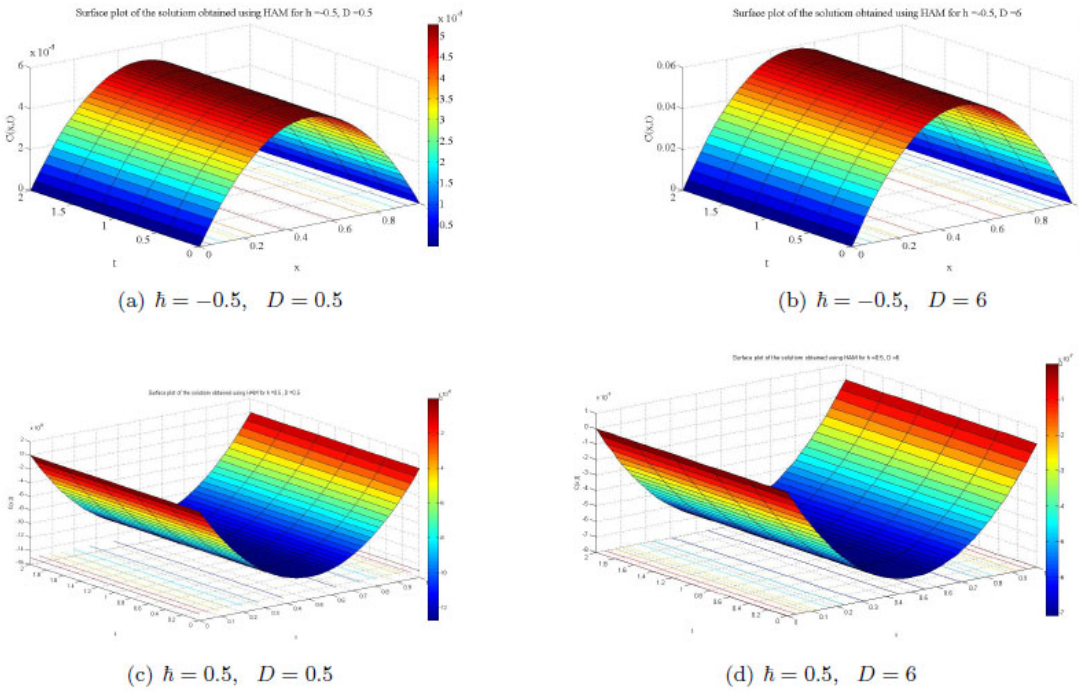

(a) $\hbar = -0.5, \quad D = 0.5$

(b) $\hbar = -0.5, \quad D = 6$

(c) $\hbar = 0.5, \quad D = 0.5$

(d) $\hbar = 0.5, \quad D = 6$

Figure 4: Surface plots of solution obtained using HAM for $\hbar = -0.5, 0, 5$ and $D = 0.5,\ 6$.

This figure shows that the energy generated in the human cell increases with time to a maximum value and then begins to decreases as it is being used to do work in the cell.

7.1 Error Control Using the Residual

In this section we discuss the error in the HAM solution obtained. It is usually very necessary to compute the error associated with approximate analytic solutions as this will indicate how the approximate solution deviates from the true solution. In the case where the exact solution is not available and cannot be obtained as in this case, the direct computation of error becomes difficult. However, the residual of the solution can be compute to show how far the approximated solution differ from the true or exact solution. Hence, one measure of the error in an approximation is given by computing the residual errors at each point.

One of the advantages of applying the homotopy analysis method(HAM) is that it gives us a way to control the convergence of solutions by choosing appropriate control parameters and auxiliary functions that would minimize error in approximate solution. It is, however, difficult to determine the error minimizing control parameters directly (Van Gorder, 2012).

The residual function for the solution (37) at each point $(x, t) \in \Omega$, is given as

$$Res(x) = \frac{\partial C_N}{\partial t} - k_1 \frac{\partial^2 C_N}{\partial x^2} + k_2 C_N - k_3(2 - k_4 t)^2, \tag{38}$$

and the squared residual error is given as

$$E_N(\hbar) = \int_0^1 (Res(x))^2 dx. \tag{39}$$

The figure below (5) shows the plot of residual error for the case when t=2, D =6 and $\hbar = 0.1$. The values are given in (1)

Table 1: Table showing the values of residual error for HAM solution

x	$\hbar$
0.00	0.00096598840
0.01	0.00096598880
0.02	0.00096598920
0.53	0.00096599780
0.95	0.00096599020
0.98	0.00096598920
0.99	0.00096598880
1.00	0.00096598840

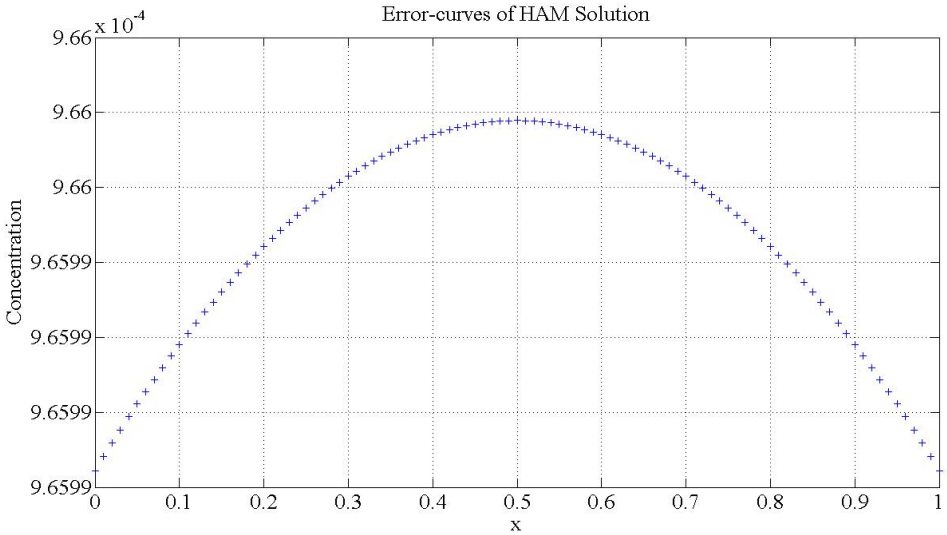

Figure 5: Plot of the Residual error of HAM solution for $\hbar = -0.1$ and diffusion coefficient, $D = 6$

.

8 Solution of Fractional Derivative model via HAM

In this section we obtain the solution to the time-fractional derivative model of energy generation in mitochondria. The fractional derivative operator use in this is the Caputo fractional derivative, which has been defined above. Using the Homotopy Analysis Method we obtain an analytic solution to the equation (16) - (17). Consider the boundary value problem

$$\begin{cases} \frac{\partial^\alpha C}{\partial t^\alpha} - k_1 \frac{\partial^2 C}{\partial x^2} + k_2 C - k_3 (V_0 - k_4 t)^2 = 0, \quad \alpha \in (0,1] \\ C(0,t) = 0, \quad C(1,t) = c_0. \end{cases} \tag{40}$$

In order to use HAM, we choose the linear operator to be

$$L[\phi(x,t;q)] = \frac{\partial^2 \phi}{\partial x^2} = D^2.$$

The inverse operator is defined as

$$L^{-1} = \int_0^x \int_0^s d\tau ds.$$

The zeroth order deformation equation is given as

$$(1-q)L[\phi(x,t;q)-\phi_0(x,t;q)] = q\hbar H(x,t)N[\phi(x,t;q)], \tag{41}$$

where $q \in [0,1]$ and $\phi_0(x,t;q)$ is the initial guess function. The operator $N[\phi(x,t;q)]$ is given as

$$N = \frac{\partial^\alpha C}{\partial t^\alpha} - k_1\frac{\partial^2 C}{\partial x^2} + k_2 C - k_3(V_0 - k_4 t)^2$$

subject to

$$\phi(0,t) = 0 \quad \text{and} \quad \phi(1,t) = \phi_0.$$

Note that when $q = 0$, the zeroth order deformation equation leads to $\phi(x,t;q) = \phi_0(x,t;q)$ and when $q = 1$, it leads to

$$\frac{\partial^\alpha C}{\partial t^\alpha} - k_1\frac{\partial^2 C}{\partial x^2} + k_2 C - k_3(V_0 - k_4 t)^2 = 0.$$

This implies that $\phi(x,t;0) = \phi_0(x,t)$ and $\phi(x,t;1) = C(x,t)$ which is the solution to the equation

$$N[\phi(x,t;1)] = 0.$$

On setting the initial approximation function to be $\phi_0(x,t) = C_0$, the solution to the boundary value problem (40) can be expressed in Taylor series as

$$\phi(x,t;1) = C_0(x,t) + \sum_{m=1}^{\infty} C_m(x,t), \tag{42}$$

which implies that

$$C(x,t) = C_0(x,t) + \sum_{m=1}^{\infty} C_m(x,t)$$

which converges when the linear operator L, the initial approximation function, $\phi_0(x,t)$, the auxiliary parameter $\hbar$ and the auxiliary function, $H(x,t)$ are chosen correctly.

The solution $C(x,t)$ is obtained from the mth order deformation equation

$$L[C_m(x,t) - \chi_m C_{m-1}(x,t)] = \hbar H(x,t) R_m(C_{m-1}(x,t)), \qquad m \geq 1 \tag{43}$$

subject to the boundary condition

$$C_m(0,t) = C_m(1,t) = 0, \tag{44}$$

where

$$\begin{aligned} R_m(C_{m-1}) &= \frac{1}{(m-1)!}\frac{\partial^{m-1}}{\partial q^{m-1}} N[\phi(x,t;q)]\Big|_{q=0} \\ &= \frac{\partial^\alpha}{\partial t^\alpha} C_{m-1} - k_1\frac{\partial^2}{\partial x^2} C_{m-1} + k_2 C_{m-1} - (1-\chi_m)k_3(V_0 - k_4 t)^2. \end{aligned}$$

We chose the auxiliary function $H(x,t) = 1$ and apply the inverse operator, L^{-1}, on the mth order deformation equation to get

$$\begin{aligned} C_m(x,t) &= \chi_m C_{m-1}(x,t) + \hbar \int_0^x \int_0^s [R_m(C_{m-1}(\tau,t))]\, d\tau(ds) \\ &= \chi_m C_{m-1}(x,t) \\ &\quad + \hbar \int_0^x \int_0^s \left[\frac{\partial^\alpha}{\partial t^\alpha} C_{m-1} - k_1\frac{\partial^2}{\partial x^2} C_{m-1} + k_2 C_{m-1} - (1-\chi_m)k_3(V_0 - k_4 t)^2\right] d\tau ds \\ &\quad + c_1 + c_2 x, \end{aligned} \tag{45}$$

where the constants c_1 and c_2 are obtained by applying the initial conditions (44) to get

$$\begin{aligned} c_1 &= -\chi_m C_{m-1}(0,t) \quad \text{and} \\ c_2 &= \chi_m C_{m-1}(0,t) \\ &\quad -\hbar \int_0^1 \int_0^s \left[\frac{\partial}{\partial t} C_{m-1} - k_1 \frac{\partial^2}{\partial x^2} C_{m-1} + k_2 C_{m-1} - (1-\chi_m) k_3 (V_0 - k_4 t)^2 \right] d\tau ds \\ &\quad -\chi_m C_{m-1}(1,t). \end{aligned}$$

Thus the we have

$$\begin{aligned} C_m(x,t) &= \chi_m C_{m-1}(x,t) + \hbar \int_0^x \int_0^s \left[R_m(C_{m-1}(\tau,t)) \right] d\tau(ds) \\ &= \chi_m C_{m-1}(x,t) \\ &\quad +\hbar \int_0^x \int_0^s \left[\frac{\partial^\alpha}{\partial t^\alpha} C_{m-1} - k_1 \frac{\partial^2}{\partial x^2} C_{m-1} + k_2 C_{m-1} - (1-\chi_m) k_3 (V_0 - k_4 t)^2 \right] d\tau ds \\ &\quad -\chi_m C_{m-1}(0,t) + \left[\chi_m C_{m-1}(0,t) - \chi_m C_{m-1}(1,t) \right] x \\ &\quad -\hbar x \int_0^1 \int_0^s \left[\frac{\partial^\alpha}{\partial t^\alpha} C_{m-1} - k_1 \frac{\partial^2}{\partial x^2} C_{m-1} + k_2 C_{m-1} - (1-\chi_m) k_3 (V_0 - k_4 t)^2 \right] d\tau ds. \quad (46) \end{aligned}$$

The solution to the original equation (40) is therefore given as

$$C(x,t) = c_0 + \sum_{m=1}^{\infty} C_m(x,t). \quad (47)$$

9 Graphical Display of HAM solution for Fractional Derivative Model

In order for the series solution obtained by HAM to converge, the auxiliary control parameter must be chosen within the region of convergence of the solution. The admissible region of convergence is usually the flat region in the $\hbar$-curve. The $\hbar$-curve for the fractional -time model at order 3 approximation and at $x = 0.2$, $t = 2$ and $\alpha = 0.5$ is shown in figure 6(a). From the graph, the admissible region of convergence is $[-1.26, 0) \cup (0, 1.08]$. From this interval a suitable optimal value is chosen that guarantees the convergence of the solution obtained by HAM.

As in the case for integer derivative model, we choose the auxiliary control parameter $\hbar = -1$ (since -1 is in the interval of convergence) and consider an BVP with diffusion coefficient $D = \frac{1}{2}$. Substituting these values into a MATLAB program yield the following analytic approximate solution.

$$\begin{aligned} C_0(x,t) &= 2 \\ C_1 &= 0.0000000603t^2x^2 - 0.0000000603t^2x - 0.0000153tx^2 + 0.0000153tx - 157.0x^2 \\ &\quad +157.0x + 2.0 \\ C_2 &= 2422.0x + 0.00000014t^2x^2 + 0.00000158t^2x^3 - 88.7t^(1/2)x^2 - 0.00000079t^2x^4 \\ &\quad +59.1t^(1/2)x^3 - 0.00000574t^(3/2)x^2 + 0.00000382t^(3/2)x^3 + 0.000000182t^(5/2)x^2 \\ &\quad -0.000000121t^(5/2)x^3 + 0.000235tx - 0.0000354tx^2 - 0.00000093t^2x - 0.00040tx^3 \\ &\quad +29.6t^(1/2)x + 0.00020tx^4 + 0.00000191t^(3/2)x \\ &\quad -0.00000605t^(5/2)x - 365.0x^2 - 4122.0x^3 + 2066.0x^4 + 4.0 \end{aligned}$$

More solutions were are obtained using MATLAB and the corresponding plot of the solution by HAM is shown in figure 6(b)

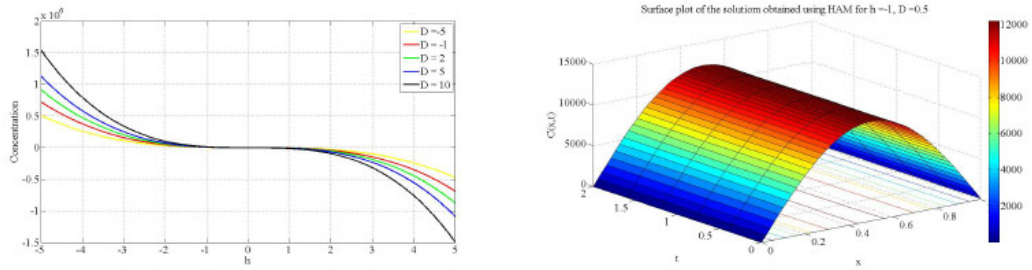

(a) $\hbar$ - Curves for different values of D at $x = 0.2$ $t = 2$ (b) Surface plots of solution via HAM for $D = \frac{1}{2}$ and $\hbar = -1$

Figure 6: Surface plots of solution obtained using HAM for $\hbar = -0.5, 0, 5$ and $D = 0.5,\ 6$.

This figure shows that the energy generated in the human cell increases with time to a maximum value and then begins to decreases as it is being used to do work in the cell.

10 Discussions and Results

A mathematical model of energy generation in human cell was introduced and studied. An approximate analytic solution to the integer order model was obtained using the Homotopy analysis Method(HAM). Surface plots of the solution obtained is presented in figures 3, and 4 for different values of the diffusion coefficient and convergence control parameter. As shown in the plots, the concentration of glucose increases as long as the control parameter stays within the range $[-1, 0)$. This range serves as the appropriate range of convergence of the solution obtained using the HAM. Outside the convergence range, the solution is no longer physically realistic.

As seen from the plots, the concentration of energy generated represented by $C(x, t)$ increases with time until it gets to a maximum level and then decreases which is an indication of usage of the energy by the cells to do work. The higher the coefficient of diffusion the more energy is generated.

The fractional-time model shows a similar result. However, in comparison with the integer partial derivative model, the energy generated using the integer model is higher than that generated by the fractional-time model. this is an advantage of the integer model over the fractional-time model. The cause of this lower energy generation may be attributed to the natural and well known chaotic behaviour of fractional models. The lower energy generated may also be due to the fewer number of approximation of the solution obtained.

11 Conclusion

The integer and fractional-time derivative models of energy generation in human body has been studied and the solution to the given models were obtained using Homotopy Analysis Method. The research shows that the amount of glucose intake that enters into the body system moves into the mitochondria matrix in oxidized form at a distance very small depending on the initial volume and concentration of glucose supplied to the blood and cells. In the mitochondria, energy in form of ATP is being generated depending on the position of interest and much as work that is being done by body system. The volume of the glucose in the mitochondria cortex and the energy generated in the form of ATP reduce with time.

The novelty in this research is the application of fractional derivative to the investigation of the generation of energy in human body by human cells. Moreover, the application of the novel Homotopy Analysis Method to fractional partial differential equation is also worthy of note.

12 Acknowledgment:

This research is sponsored by TETFUND Nigeria under the IBR funding with project number:TETFUND/DR&D/CE/UNI/NSUKKA/RP/VOL.I

References

Abbasbandy, S. (2006). The application of homotopy analysis method to nonlinear equations arising in heat transfer. *Physics Letters A*, *360*(1), 109-113.

Adomian, G., Adomian, G. (1984). A global method for solution of complex systems. *Math.Model*, 5, 521-568.

Ahmad, R. S. (2015). *An analytical solution of the fractional Navier-Stokes equation by residual power series method. Zarqa University.* PhD thesis, Doctoral dissertation, 10-90.

Akinyemi, L. (2019). q-homotopy analysis method for solving the seventh-order time-fractional lax's Korteweg–de Vries and sawada–kotera equations. *Computational and Applied Mathematics*, *38*(4), 1–22.

Akinyemi, L., Huseen, S. N. (2020). A powerful approach to study the new modified coupled korteweg–de vries system. *Mathematics and Computers in Simulation*, 177, 556–567.

Akinyemi, L., Iyiola, O. S. (2020a). Exact and approximate solutions of time-fractional models arising from physics via shehu transform. *Mathematical Methods in the Applied Sciences*, *43*(12), 7442–7464.

Akinyemi, L., Iyiola, O. S. (2020b). A reliable technique to study nonlinear time-fractional coupled korteweg–de vries equations. *Advances in Difference equations*, *2020*(1), 1–27.

Arikoglu, A., Ozkol, I. (2007). Solution of fractional differential equations by using differential transform method. *Chaos, Solitons & Fractals*, *34*(5), 1473–1481.

Ayeni, R. O., Okedoye, A. M., Popoola, A. O., & Ayodele, T. O. (2005). Effect of radiation on the critical frank – kamenetskii parameter of thermal ignition in a combustible gas containing fuel droplets. *Journal of the Nigerian Association of Mathematical Physics*, 9, 217–220.

Baleanu, D., Güvenç, Z.B., & Machado, J. T. (Eds.). (2010). *New trends in nanotechnology and fractional calculus applications* (Vol. 10, pp. 978-90). New York: Springer.

Baleanu, D., Wu, G.-C., & Zeng, S.-D. (2017). Chaos analysis and asymptotic stability of generalized caputo fractional differential equations. *Chaos, Solitons & Fractals*, 102, 99–105.

Chakraverty, S., Mahato, N., Karunakar, P., & Rao, T. D. (2019). *Advanced numerical and semi-analytical methods for differential equations.* John Wiley & Sons.

Didi, F., Chaouche, M.S., Amari, M., Guezmir, A., Belhenniche, K., & Chellali, A. (2023). Design and simulation of grid-connected photovoltaic system's performance analysis with optimal control of maximum power point tracking MPPT based on artificial intelligence. *Tobacco Regulatory Science* (TRS), 1074-1098.

Diethelm, K., Ford, N.J. (2002). Analysis of fractional differential equations. *Journal of Mathematical Analysis and Applications, 265*(2), 229-248.

Ejikeme, C., Mbah, G., & Oyesanya, M. (2011). Energy generation in human body by human cell. *Journal of Nigerian Association of Mathematical Physics*, 19, 99–106.

Ejikeme, C., Oyesanya, M., Agbebaku, D., & Okofu, M. (2018). Solution to nonlinear duffing oscillator with fractional derivatives using homotopy analysis method (HAM). *Global Journal of Pure and Applied Mathematics*, *14*(10), 1363–1388.

Ejikeme, C. L. (2006). Energy generation in human body by human cells. Master's thesis, Department of Mathematics, University of Nigeria Nsukka.

Ghalandari, M., Ziamolki, A., Mosavi, A., Shamshirband, S., Chau, K.-W., & Bornassi, S. (2019). Aeromechanical optimization of first row compressor test stand blades using a hybrid machine learning model of genetic algorithm, artificial neural networks and design of experiments. *Engineering Applications of Computational Fluid Mechanics*, *13*(1), 892–904.

Harris, D.A., Das, A.M. (1991). Control of mitochondrial ATP synthesis in the heart. *Biochemical journal, 280*(Pt 3), 561.

Hastings, S.P., McLeod, J.B. (2011). *Classical methods in ordinary differential equations: with applications to boundary value problems* (Vol. 129). American Mathematical Soc.

He, J.-H. (1999). Homotopy perturbation technique. *Computer methods in applied mechanics and engineering*, *178*(3-4), 257–262.

Hetmaniok, E., Słota, D., Trawiński, T., & Wituła, R. (2014). Usage of the homotopy analysis method for solving the nonlinear and linear integral equations of the second kind. *Numerical Algorithms*, 67, 163–185.

Hickman, F.N., Hickman, C.P. (1997). *Biology of Animals.* W C B/McGraw-Hill, 7th Edition.

Hoan, L. V. C., Akinlar, M. A., Inc, M., Gómez-Aguilar, J., Chu, Y.-M., & Almohsen, B. (2020). A new fractional-order compartmental disease model. *Alexandria Engineering Journal*, *59*(5), 3187–3196.

Iyiola, O. S. (2015). On the solutions of non-linear time-fractional gas dynamic equations: an analytical approach. *International Journal of Pure and Applied Mathematics*, *98*(4), 491–502.

Jafarian-Namin, S., Goli, A., Qolipour, M., Mostafaeipour, A., & Golmohammadi, A.-M. (2019). Forecasting the wind power generation using box–jenkins and hybrid artificial intelligence: A case study. *International journal of energy sector management.*

Kexue, L., Jigen, P. (2011). Laplace transform and fractional differential equations. *Applied Mathematics Letters*, *24*(12), 2019–2023.

Kilbas, A.A.A., Srivastava, H.M., & Trujillo, J.J. (2006). *Theory and applications of fractional differential equations.* volume 204, Elsevier Science Limited.

Korla, K., Mitra, C. K. (2014). Modelling the krebs cycle and oxidative phosphorylation. *Journal of Biomolecular Structure and Dynamics*, *32*(2), 242–256.

Korzeniewski, B. (1996). Simulation of oxidative phosphorylation in hepatocytes. *Biophysical chemistry*, *58*(3), 215–224.

Korzeniewski, B. (1998). Regulation of atp supply during muscle contraction: theoretical studies. *Biochemical Journal*, *330*(3), 1189–1195.

Kumar, A., Kumar, S., & Singh, M. (2016). Residual power series method for fractional Sharma-Tasso-Olever equation. *Commun. Numer. Anal*, 10, 1–10.

Kumar, D., Seadawy, A.R., & Joardar, A. K. (2018). Modified Kudryashov method via new exact solutions for some conformable fractional differential equations arising in mathematical biology. *Chinese Journal of Physics*, *56*(1), 75–85.

Kumar, D., Singh, J., & Baleanu, D. (2017). A new analysis for fractional model of regularized long-wave equation arising in ion acoustic plasma waves. *Mathematical Methods in the Applied Sciences*, *40*(15), 5642–5653.

Liang, S., Jeffrey, D. J. (2009). Comparison of homotopy analysis method and homotopy perturbation method through an evolution equation. *Communications in Nonlinear Science and Numerical Simulation*, *14*(12), 4057–4064.

Liao, S. (1992). *The proposed homotopy analysis technique for the solution of nonlinear problems.* PhD thesis, PhD thesis, Shanghai Jiao Tong University.

Liao, S. (2003). *Beyond Perturbation: Introduction to the Homotopy Analysis Method.* Chapman and Hall CRC Press, Boca Raton.

Liao, S., Tan, Y. (2007). A general approach to obtain series solutions of nonlinear differential equations. *Stud.Appl.Math.*, 119, 297–355.

Liu, J.-G., Yang, X.-J., Feng, Y.-Y., & Zhang, H.-Y. (2020). Analysis of the time fractional nonlinear diffusion equation from diffusion process. *Journal of Applied Analysis & Computation*, *10*(3), 1060–1072.

Mainardi, F. (2010). *Fractional calculus and waves in linear viscoelasticity: an introduction to mathematical models.* World Scientific.

Mastroberardino, A. (2011). Homotopy analysis method applied to electrohydrodynamic flow. *Communications in Nonlinear Science and Numerical Simulation*, *16*(7), 2730–2736.

McMurry, J., Castellion, M.E., Ballantine, D.S., Hoeger, C.A., & Peterson, V.E. (1996). *Fundamentals of general, organic, and biological chemistry.* Prentice Hall, 6th ed.

Molajou, A., Nourani, V., Afshar, A., Khosravi, M., & Brysiewicz, A. (2021). Optimal design and feature selection by genetic algorithm for emotional artificial neural network (eann) in rainfall-runoff modeling. *Water Resources Management*, *35*(8), 2369–2384.

Nabipour, N., Dehghani, M., Mosavi, A., & Shamshirband, S. (2020). Short-term hydrological drought forecasting based on different nature-inspired optimization algorithms hybridized with artificial neural networks. *IEEE Access*, 8, 15210–15222.

Nasrolahpour, H. (2013). A note on fractional electrodynamics. *Communications in Nonlinear Science and Numerical Simulation*, *18*(9), 2589–2593.

Otugene, V. B. (2012). Mathematical modeling of energy generation in mitochondria. Master's thesis, Department of Mathematics University of Nigeria, Nsukka.

Poblubny, I. (1999). *Fractional Differential Equations.* Academic Press, San Diego.

Ray, S. S., Bera, R. (2005). An approximate solution of a nonlinear fractional differential equation by adomian decomposition method. *Applied Mathematics and Computation*, *167*(1), 561–571.

Sajid, M., Hayat, T. (2008). Comparison of ham and hpm methods in nonlinear heat conduction and convection equations. *Nonlinear Analysis: Real World Applications*, *9*(5), 2296–2301.

Senol, M. (2020). Analytical and approximate solutions of (2+ 1)-dimensional time-fractional burgers-kadomtsev-petviashvili equation. *Communications in Theoretical Physics*, *72*(5), 055003.

Şenol, M., Dolapci, I.T. (2016). On the perturbation–iteration algorithm for fractional differential equations. *Journal of King Saud University-Science*, *28*(1), 69–74.

Song, L., Zhang, H. (2007). Application of homotopy analysis method to fractional kdv–burgers–kuramoto equation. *Physics Letters A*, *367*(1-2), 88–94.

Sun, H., Zhang, Y., Baleanu, D., Chen, W., & Chen, Y. (2018). A new collection of real world applications of fractional calculus in science and engineering. *Communications in Nonlinear Science and Numerical Simulation*, 64, 213–231.

Tarasov, V. E. & Tarasova, V. V. (2017). Time-dependent fractional dynamics with memory in quantum and economic physics. *Annals of Physics*, 383, 579–599.

Tuan, N. H., Baleanu, D., Thach, T. N., O'Regan, D., & Can, N. H. (2020). Final value problem for nonlinear time fractional reaction–diffusion equation with discrete data. *Journal of Computational and Applied Mathematics*, 376, 112883.

Van Gorder, R. A. (2012). Control of error in the homotopy analysis of semi-linear elliptic boundary value problems. *Numerical Algorithms*, 61, 613–629.

Yi-Fei, P. (2007). Fractional differential analysis for texture of digital image. *Journal of Algorithms & Computational Technology*, *1*(3), 357–380.

Yildirim, A. (2009). An algorithm for solving the fractional nonlinear schrödinger equation by means of the homotopy perturbation method. *International Journal of Nonlinear Sciences and Numerical Simulation*, *10*(4), 445–450.

Zhang, Y., Pu, Y., Hu, J., & Zhou, J. (2012). A class of fractional-order variational image inpainting models. *Appl. Math. Inf. Sci*, *6*(2), 299–306.